Bonding and Valence Electron Distributions in Molecules. Experimental Determination of Aspherical Electron Charge Density in Tetracyanoethylene Oxide[1]

D. A. Matthews* [2] **and G. D. Stucky**

Contribution from the School of Chemical Sciences and Materials Research Laboratory, University of Illinois, Urbana, Illinois 61801.
Received January 8, 1971

Abstract: Combined X-ray and neutron diffraction studies have been used to determine the thermally averaged aspherical electron charge distribution in tetracyanoethylene oxide. The densities in the plane of the ring are discussed in terms of semiempirical and SCF–LCAO–MO calculations which have been made on similar strained three-membered-ring molecules. The vector from a ring carbon to the maximum for the difference density in the endocyclic C–C bonding region is shown to form an angle of 12° with the internuclear axis, while the density in the C–O bond region is obscured by the tailoff from an accumulation of electron density in the middle of the ring. Difference Fourier and valence Fourier sections through a number of chemically interesting parts of the molecule are presented and discussed. Differences between the X-ray and neutron thermal and positional parameters are discussed in terms of the bias introduced in the X-ray refinement by the spherical atom scattering factor formalism.

Considerable interest in the structure and chemistry of small strained ring molecules is evidenced by the large amount of work that continues to be published in this area. In the preceding paper,[3] a detailed study of the crystal structure of tetracyanoethylene oxide (TCEO) was reported. The parent compound, ethylene oxide, and its carbon analog, cyclopropane, have been widely studied both experimentally and theoretically in an attempt to describe the bonding features of the ring. Interest has been centered principally on whether or not the "bent bond" model first proposed by Coulson and Moffitt is at least a qualitatively correct description of the bonding in strained ring systems.[4] The model predicts that for cyclopropane the region of greatest electron density is outside the ring rather than along the C–C internuclear axis.

In principle, X-ray scattering from crystals inherently contains a wealth of information concerning the distribution of electron density. However, the spherical atom scattering factor formalism used in routine crystal structure analysis obscures or eliminates the details of these distributions. Recently, Coppens, *et al.*, have used X-ray and neutron diffraction techniques to obtain experimental confirmation that accurate X-ray scattering data does contain useful information concerning deviations of atoms in molecules from spherical symmetry.[5,6] This work represents an extension of these techniques to TCEO for the purpose of analyzing the electronic charge density in a strained ring molecule.

Theoretical Background

When the diffraction data have been corrected for extinction, absorption, and multiple reflection, the kinematic approximation holds and the time-averaged scattering of an incident wave by a crystal is proportional to the magnitude of the structure factor squared

$$I(\mathbf{S}) \sim |F_{hkl}|^2 = \sum_{j=1}^{N}\sum_{j'=1}^{N} f_j(\mathbf{S}) f_{j'}(\mathbf{S}) \times \exp 2\pi i \mathbf{S}\cdot(\mathbf{r}_j - \mathbf{r}_{j'}) T_j(\mathbf{S}) T_{j'}(\mathbf{S}) \quad (1)$$

where the double summation is over all N atoms in the crystal, f_j is the scattering factor for the jth atom, T_j is the Debye–Waller factor, and $\mathbf{r}_j$ is the position vector of the jth atom in the unit cell. If $\mathbf{s}_0$ and $\mathbf{s}$ are unit vectors parallel to the incident and diffracted beams, respectively, then $\mathbf{S} = 2\pi/\lambda\,(\mathbf{s} - \mathbf{s}_0)$. The inadequacies of the spherical atom scattering factor formalism have been noted earlier. Neutrons are scattered by the atomic nuclei which appear as point scatterers to neutrons with wavelengths comparable to internuclear separations. When the thermal and positional parameters are determined from a neutron diffraction experiment, they are not biased by any assumed form of the scattering factor. These parameters can then be used to calculate phases for the observed X-ray structure factors. A difference Fourier series can then be constructed according to

$$\rho_{X-N}(x, y, z) = (1/V)\sum_{hkl}(F_X - F_N) \times \exp[-2\pi i(hx + ky + lz)] \quad (2)$$

where F_X is the observed X-ray structure factor with the phase of F_N and F_N is the structure factor whose phase and amplitude are calculated from the neutron thermal and positional parameters and spherical atom scattering factors. The resultant function ρ_{X-N} represents the redistribution of charge density in going from the isolated atoms to the molecule.

In the present work, we have assumed that the Gaussian Debye–Waller form for the thermal smearing function in (1) is an acceptable choice. This formalism can only describe harmonic rectilinear motion. The real thermal motion may have anharmonic or harmonic nonrectilinear components or both. Anharmonic contributions to the Debye–Waller factor have been dis-

(1) This research was supported by the Advanced Research Projects Agency under Contract No. HC 15-67-C-0221, by the National Science Foundation, and by the donors of the Petroleum Research Fund, administered by the American Chemical Society.
(2) University of Illinois Graduate Fellow, 1967–1969; American Chemical Society–Petroleum Research Fund Graduate Fellow, 1969–1970.
(3) D. A. Matthews, J. Swanson, M. H. Mueller, and G. D. Stucky, *J. Amer. Chem. Soc.*, **93**, 5945 (1971).
(4) C. A. Coulson and W. E. Moffitt, *Phil. Mag.*, **40**, 1 (1949).
(5) P. Coppens, *Science*, **158**, 1577 (1967).
(6) P. Coppens, T. M. Sabine, R. G. Delaplane, and J. A. Ibers, *Acta Crystallogr., Sect. B*, **25**, 2351 (1965).

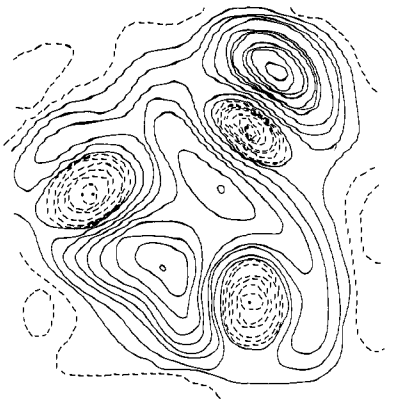

Figure 1. The difference function ρ_{X-N} calculated in the plane of the ethylene oxide ring. Negative and zero contours are broken. The contours are at 0.05-e/Å^3 increments.

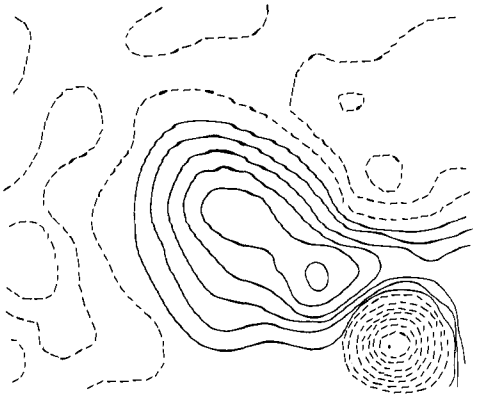

Figure 2. The difference density perpendicular to the C–O bond through the midpoint. The scale is the same as in Figure 1.

cussed by Willis,[7] and their importance has been demonstrated in an accurate neutron diffraction investigation of barium fluoride.[8] Anharmonic effects are most pronounced at high values of sin θ/λ,[7] where θ is the Bragg angle and λ is the wavelength of the incident radiation. This means that in Fourier maps the main distortions due to artifacts in the structure factors calculated in the harmonic rectilinear approximation will occur at or very close to the atomic nucleus. The regions of interest in this work are those associated with valence structure and are considerably removed from the nuclear positions. The main harmonic nonrectilinear motion in TCEO is molecular liberation.[3] The inability of the Gaussian formalism to satisfactorily approximate this type of motion is well known. Johnson has developed a statistical approach to thermal motion which makes no prejudgment concerning the form of the smearing function.[9] Unfortunately, the description is so general as to require an often prohibitively large number of parameters. In structures where the number of data are sufficient to greatly overdetermine the least-squares problem, this formalism will be valuable. When such information is available, it will be possible to study the effect which these motions have on electron density maps.

A second assumption is that the relative contribution of thermal diffuse scattering (TDS) to the Bragg intensity is nearly the same in both the X-ray and neutron experiment.[6] Cochran has shown that the first-order cross section for neutron scattering from acoustic phonons (which makes the primary contribution to TDS at room temperature) reduces to the X-ray result provided that the neutrons are faster than the speed of sound in the crystal.[10] In our experiment, this is certainly the case since the speed of the thermal neutrons was greater than 3000 m/sec.

Finally, in order to justify the convolution of a nuclear thermal smearing function onto static electron distributions, we assume that the adiabatic approximation holds so that the electron coordinates are the same for all positions of the nuclei. This approximation is quite accurate.

(7) B. T. M. Willis, *Acta Crystallogr., Sect. A*, **25**, 277 (1969).
(8) M. J. Cooper, K. D. Rouse, and B. T. M. Willis, *ibid., Sect. A*, 24, 484 (1968).
(9) C. K. Johnson, *ibid., Sect. A*, **25**, 187 (1969).
(10) W. Cochran, *Rep. Progr. Phys.*, **26**, 1 (1963).

Difference Fourier Sections

The structure factors calculated with neutron parameters and spherical atom scattering factors F_N can be scaled to the observed X-ray structure amplitudes F_X with the scale factor derived from the X-ray refinement. However, this scale factor is expected to be in error owing to the spherical atom approximation. Coppens has suggested varying the scale factor in a least-squares fit of F_N to F_X but holding the positional and thermal parameters at their neutron values.[6] This was the procedure used here. The new scale factor k (where $kF_{calcd} = F_{obsd}$) was found to have decreased by 6.0%. The spherical atom scattering factors for all calculations were taken from Hansen, *et al.*[11]

Figure 1 shows the difference Fourier synthesis, ρ_{X-N}, calculated over all observed X-ray reflections and evaluated in the plane of the ethylene oxide ring. The atoms show up as negative depressions since the spherical atom model has placed excess electron density in these regions at the expense of bonding and lone-pair density which then appear in the difference map as regions of positive electron density. The density in the C–C internuclear regions is seen to attain a maximum of about 0.45 e/Å^3 and to be displaced about 0.16 Å normal to the internuclear axis. This corresponds to an angle of 12° as measured from the carbon nuclear position and gives strong support for the existence of bent bonds in strained three-membered ring molecules. The bend in the C–O bond is apparently obscured by the tail-off of the broad maxima attained near the center of the ethylene oxide ring. For this peak the maximum density of about 0.35 e/Å^3 is reached at a point equidistant from each carbon but shifted toward the more electronegative oxygen atom.

In Figure 2 is shown the difference Fourier section perpendicular to the C–O bond through the midpoint. The negative area represents the other ring carbon, and the gradual buildup in the area above and to the right of the carbon is due to an exocyclic C–C bond. The electron buildup inside the ring is clearly evident. Note that the 0.25-e/Å^3 contour is dumbbell-shaped due to the additional accumulation of density near the C–O axis. The maximum density in this region occurs at a perpendicular distance of about 0.10 Å from the C–O internuclear axis, but this density is only 0.01 e/Å^3 greater than that at the midpoint of the bond.

(11) H. P. Hansen, F. Herman, J. O. Lea, and S. Skillman, *Acta Crystallogr.*, **17**, 1040 (1964).

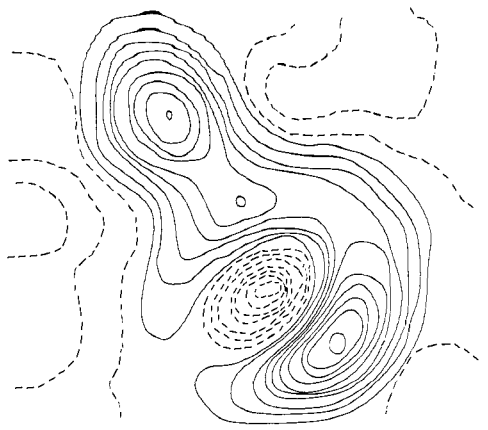

Figure 3. The difference density perpendicular to the endocyclic C–C bond and passing through the oxygen. The scale is the same as in Figure 1.

The semiempirical Coulson–Moffitt[4] and Walsh[12] models have been widely used to explain the physical and chemical properties of three-membered ring molecules. In view of the interest in these models and the widespread controversy concerning which provides the more useful description of the bonding, it is worthwhile to look at their relation to the present results. In addition, several of the SCF–LCAO–MO calculations recently reported for cyclopropane and some heterocyclic derivatives will be briefly discussed.[13,14] The experimental densities given here are convoluted onto a history of thermal motion and so are not quantitatively comparable to theoretical results, however, for valence densities these differences are not severe.

The Walsh model postulates the overlap of three p orbitals to form a bonding region exterior to the ring into which four electrons are placed. The remaining two electrons, not involved in localized bonding to exocyclic atoms, are associated with a molecular orbital formed by the overlap of three sp^2 hybridized orbitals, one from each carbon center. This internal molecular orbital leads to a buildup of density in the center of the ring. The Coulson–Moffitt approach describes each C–C bond in terms of an overlap of approximately sp^5 hybrid orbitals on adjacent carbons producing a bent bond. Although the two models are often discussed as providing alternative approaches to bonding in strained rings, the descriptions are much less divergent than one would expect from the different starting assumptions in each case. Coulson and Moffitt have given contours of equal electron density for the six bonding electrons in the plane of the cyclopropane ring which they derived by superposition of the individual density in each bent bond.[4] The results show a density maximum in the center of the ring which is somewhat higher than that in the bonding region, and the character of an individual bent bond is highly obscured. Although no detailed contour maps have been published for the Walsh model, this description should give rather similar results. Recently, SCF calculations with minimal STO basis sets, employing the SCF Roothaan scheme, were reported for a number of heterocyclic three-membered ring systems.[13] No bond density contours were given for ethylene oxide, but the electron density maps for the C–C and C–N bonds in aziridine were reported. These localized orbitals show distinct maxima displaced from the internuclear axis, in agreement with the bent bond concept. We have constructed a total ring electron density map by superimposing two C–N bonds with the C–C bond. These results also predict a buildup of density in the middle of the ring which obscures the contribution of the individual bond.

If the aggregate electron distribution in the ring is viewed as the superposition of three density diagrams, one describing each bond, it would be impossible to experimentally separate out the extent to which each bond contributed to the total distribution, and the nature or even the existence of bent bonds would remain questionable. However, in the ethylene oxide ring the greater electronegativity of the oxygen atom relative to carbon causes a shift in the centroid of the charge in the C–O bonding regions away from the carbons. In this way the C–C bond is considerably more isolated than in cyclopropane and the bend in the individual bond is clearly evident. The actual observed angle of the bend is less significant since this will depend on how much of the total electron density is subtracted out in the particular type of difference map under investigation and the extent to which the bond is really isolated in a molecular orbital sense from the effects of density in other parts of the ring. For example, the buildup of density in the center of the ring discussed above will tend to move the C–C bond maximum toward the internuclear axis and decrease the angle of bend.

These results are to be compared with a recent SCF–LCAO–MO calculation on cyclopropane.[14] The ring bonds are found to be built up from three MO's, one which provides electron density inside the ring and two which lead to high electron density outside the ring and zero density in the middle of the ring. The sum of the two distributions shows a slight depression in the center of the ring of about 15% relative to the external bonding region. The bent bond remains pronounced in the total ring electron density map. This differs from our result in that a maximum near the ring center obscures the C–O bent bond in ethylene oxide and the implication is that a similar result probably holds for cyclopropane.

Figure 1 also shows the nature of the oxygen lone-pair density in the plane of the ethylene oxide ring. The density maximum of 0.55 e/Å^3 is built up in back of the oxygen nuclear position near the line bisecting the C–C bond axis. Figure 3 presents the difference Fourier section calculated for a plane perpendicular to the endocyclic C–C bond and passing through the oxygen. The density is flattened and contracted compared to the spatial requirements for lone pairs which have been postulated in the past.[15] The contours in the neighborhood of the oxygen exhibit near mirror symmetry in the ring plane, but there is an apparent shift of density in a direction normal to the plane of the ring. This is most evident in the contours up to 0.20 e/Å^3. Free-molecule electron charge densities are known to undergo small changes on going to a condensed phase owing to interactions with neighboring molecules. Whether the observed asymmetry around the oxygen is due to this

(12) A. D. Walsh, *Trans. Faraday Soc.*, 45, 179 (1949).
(13) R. Bonaccorsi, E. Scrocco, and J. Tomasi, *J. Chem. Phys.*, 52, 5270 (1970).
(14) E. Kochanski and J. M. Lehn, *Theor. Chim. Acta*, 14, 281 (1969).
(15) F. G. Riddell, *Quart. Rev., Chem. Soc.*, 21, 364 (1967).

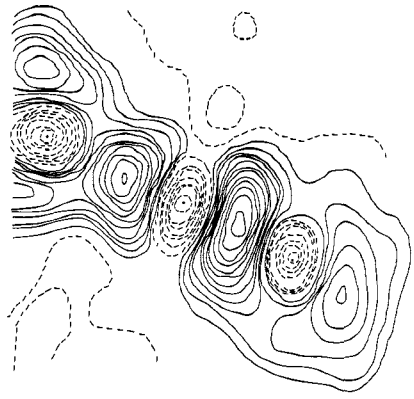

Figure 4. The difference density in the plane of the C–C–N fragment. The scale is the same as in Figure 1.

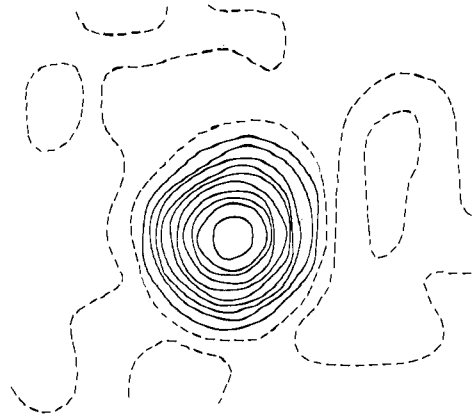

Figure 5. The difference density perpendicular to the exocyclic C-C bond through the midpoint. The scale is the same as in Figure 1.

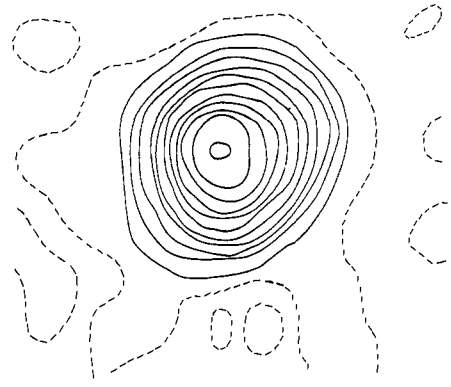

Figure 6. The difference density perpendicular to the C–N bond through the midpoint. The scale is the same as in Figure 1.

type of solid-state interaction and whether or not such effects are resolvable in our experiment must await further studies. It may be significant that the nearest-neighbor approach of oxygen to another TCEO molecule is 3.58 Å, the contact occurring with another oxygen atom directly above it. This is consistent with the observed redistribution of charge density if oxygen–oxygen repulsions are important. In most oxygen-containing molecular compounds a single-bonded oxygen atom will be imbedded too deep in the molecule to be of primary importance in determining the molecular packing. Thus very few data are available concerning an appropriate van der Waals radius. It has been suggested that this radius will be close to 1.52 Å for a cyclic ether such as ethylene oxide and that the oxygen should be significantly exposed in this case.[16] Nevertheless, the observed separation of 3.58 Å is considerably more than twice the van der Waals radius and the question still remains as to whether electron–electron repulsions could produce the observed asymmetry.

Figure 4 shows the difference Fourier function calculated in the plane of the C–C–N fragment. The C–C–N group used for this and the following calculations was C(5)–C(1)–N(1). The internal consistency of chemically similar but crystallographically independent parts of the molecule such as the four cyano groups is quite good, with most differences being no greater than 0.05 e/Å^3. A notable feature does occur in the lone-pair difference density for N(4). This density is shifted slightly to one side rather than appearing directly in back of the nitrogen as expected for a lone-pair of electrons in a predominantly sp-hybridized atomic orbital. This is probably the result of some systematic error in the neutron data, although it may be significant that the crystal packing around this nitrogen is different from that of the other three, as discussed in the preceding paper. The positive density areas appearing at either side of the ring carbon are due to bonds to another cyano group and to the other ring carbon atom. Elementary valence-bond theory would describe the hybridization at the nitrogen and exocyclic carbon as being approximately sp. The two remaining p orbitals at each center are then used to form two π bonds. The figure shows very clearly the extent to which the C–N bonding electron density is elongated in the direction of the $\rho\pi$–$\rho\pi$ overlap perpendicular to the internuclear axis. This is to be compared with the C–C density, which is described in valence-bond terms as entirely σ in character and which shows no such elongation. This point is further illustrated in Figures 5 and 6, which show sections perpendicular to the C–C and C–N bonds through their midpoints.

There is substantial accumulation of evidence which indicates that the inner 1s atomic orbitals remain unchanged in going from the atomic to a molecular environment. A Fourier synthesis of the total valence electron density can be obtained by subtracting the time-averaged $1s^2$ density from the total time-averaged density. In this valence Fourier the observed structure factors are phased as before, but the calculated structure factors are those corresponding to scattering from only the $1s^2$ time-averaged distribution. In our work we have used Clementi's basis functions[17] for the $1s^2$ atomic orbital product and calculated the scattering factor from the appropriate explicit expression given by Stewart.[18] In Figure 7, the valence charge density for the C–C–N fragment is shown. The same general features can be seen that were discussed for Figure 4.

A number of difference Fourier sections ρ_{X-N} were calculated parallel to those shown in Figures 5 and 6 at small increments in directions toward the C and N atoms, respectively. The interesting fact which emerged is that for all four C–N bonds the maximum in the difference density is at a point on the internuclear

(16) A. Bondi, *J. Phys. Chem.*, **68**, 441 (1964).

(17) E. Clementi, C. C. J. Roothaan, and M. Yoshimine, *Phys. Rev.*, **127**, 1618 (1962).

(18) R. F. Stewart, *J. Chem. Phys.*, **48**, 4882 (1968).

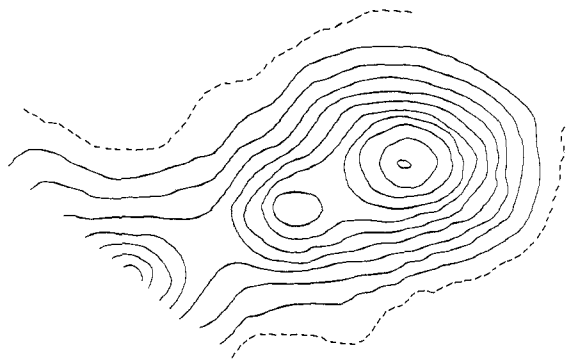

Figure 7. The valence density in the plane of the C–C–N fragment. The zero contour is broken. The contours are at 0.28-e/Å^3 increments.

axis shifted about 0.07 Å from the midpoint toward the cyano carbon. This is somewhat surprising, since a number of theoretical calculations on CN^- predict that the nitrogen is more negative than the carbon.[19,20] If the π density is more aspherical than the σ density, the above observation may represent an experimental confirmation of the π electron charge transfer from N to C predicted by Bonaccorsi, *et al.*,[20] although the distinction between the π and σ densities cannot be made from our experimental maps. In their LCAO–SCF–MO study of CN^- and HCN, they found that protonation of cyanide results in a transfer of about 15% of the gross $2p\pi$ atomic orbital population from N to C.

The nitrogen lone-pair density is clearly shown in both Figures 4 and 7. The effect of the nitrogen thermal motion on the spatial distribution of the lone pair will be rather small. In this approximation, the density distribution is in excellent agreement with the theoretical results of Bonaccorsi;[20] however, the outer contours in our work are somewhat less rounded and flatter.

Comparison of X-Ray and Neutron Positional Parameters

Table II of the preceding paper shows the X-ray and neutron positional parameters for TCEO. There are small discrepancies which may be significant for atoms in some of the cyano groups and for the oxygen. Dawson has stated that the bond lengths to terminal atoms in a molecule, when determined by X-rays, should be smaller than the value obtained by spectroscopic methods or by neutron or electron diffraction.[21] This is because the centroid of the electron density, which defines the final positional parameters for an atom in the X-ray experiment, is shifted toward the bonded neighbor. Coppens and Coulson have shown how this concept must be amended when the terminal atom contains a lone pair which will tend to shift the centroid of the distribution away from the bonded neighbor. An approximate calculation of these effects is straightforward.[22] We have assumed sp hybridization for the nitrogen and exocyclic carbon and sp^2 hybridization for the endocyclic carbon orbital used to bond to the cyano group. The integrals are of the type

$$\bar{z} = \int z\Psi^2 d\tau$$

where Ψ is the appropriate linear combination of Slater s and p orbitals when the displacement of the centroid due to a lone pair is to be calculated, and Ψ is a bonding molecular orbital between atoms A and B when the shift due to aspherical denisty in bond A–B is to be described. Overlap integrals were taken from the compilation of Mulliken, *et al.*[23] The results of these calculations for the cyano group and the oxygen are shown in Table I.

Table I. Theoretical Asphericity Shifts for Oxygen and Cyano Carbon and Nitrogen

Atom	Shifts, Å: σ density	π density	Lone pair	Net shift
N[a]	−0.011	−0.019	0.052	0.003
C[a]	−0.012	0.022		0.032
O[b]	−0.013[c]		0.037	0.011

[a] Positive z is in the direction of a vector from carbon to nitrogen. [b] Positive z is in the direction of a vector from the midpoint of the endocyclic C–C bond to the oxygen. [c] Each C–O bond assumed to make an angle of 15° with the internuclear axis.

The experimental shifts for N are not consistent. Two of the crystallographically independent nitrogen atoms are shifted in the direction of the lone pair and two are shifted toward the carbon–nitrogen bond. In addition, the displacements which range from 0.006 to 0.011 Å are in directions which make rather large angles (*ca.* 30°) with the internuclear axis. The carbon shifts cover about the same range, and the movement in three of the four cases is toward the nitrogens along the C–N bond axis as predicted in Table I. The fourth C is shifted almost perpendicular to this axis. The shortening of the C–N bond and lengthening of the exocyclic–endocyclic C–C bond in the X-ray experiment are possibly significant. On the basis of an analysis of variance, the hypothesis that the eight independent C–N distances are equivalent can be rejected at the 2.5% significance level. These differences are due in major part to the shift in the position of the cyano carbon toward the bonding density in the C–N bond. The inconsistencies of the nitrogen shifts could be dismissed as a random effect if they were very small, owing to the virtual concellation of lone-pair and bonding effects as predicted in Table I. The fact that these shifts are comparable to those of the cyano carbon suggests that these effects could be due to systematic error in the data rather than shifts in the centroid of the electron distributions.

The X-ray y positional parameter of the oxygen is seen to undergo a large shift toward lower values relative to the neutron value.[3] The total shift represents a movement of the oxygen of 0.013 (4) Å in the direction of the accumulation of lone-pair density at the back of the oxygen, as depicted in Figures 1 and 2. The agreement with the theoretical asphericity shift is quite good assuming, as a rough approximation, that the lone-pair denisty resides in sp^2 hybrids and the oxygen bonds to carbon are sp^5 hybrids bent 15° relative to the internuclear axis.

(19) G. Doggett and A. McKendrick, *J. Chem. Soc. A*, 825 (1970).
(20) R. Bonaccorsi, C. Petrongolo, E. Scrocco, and J. Tomasi, *J. Chem. Phys.*, **48**, 1500 (1968).
(21) B. Dawson, *Aust. J. Chem.*, **18**, 595 (1965).
(22) P. Coppens and C. A. Coulson, *Acta Crystallogr.*, **23**, 718 (1967).
(23) R. S. Mulliken, C. A. Rieke, D. Orloff, and H. Orloff, *J. Chem. Phys.*, 17, 1248 (1949).

Comparison of X-Ray and Neutron Thermal Parameters

The recent work of Coppens, *et al.*,[5,6] has shown that aspherical features in difference Fourier maps are obscured when only X-ray data are used, mainly because the atomic thermal parameters are increased in order to simulate bonding and lone-pair denisty which is not accounted for in the spherical atom scattering factor formalism normally used to refine a crystal structure. Similar conclusions can be drawn from our experiments by an examination of Table II, where we present the components of the anisotropic thermal tensors. It can be seen that in all cases the diagonal elements as derived from the neutron experiment are significantly smaller than the X-ray values by as much as nine combined standard deviations.

Table II. Some X-Ray and Neutron Thermal Parameters B_{ij} ($\times 10^4$)[a]

		X-Ray	Neutron	Δ	Δ/σ
O	11	110 (1)	94 (4)	16 (4)	4.0
	22	242 (3)	198 (12)	44 (12)	3.7
	33	75 (1)	66 (3)	9 (3)	3.0
	12	18 (1)	24 (6)	−8 (6)	
	13	10 (1)	0 (3)	10 (3)	
	23	24 (1)	26 (5)	−2 (5)	
C(1)	11	118 (2)	109 (4)	9 (4)	2.3
	22	196 (3)	168 (9)	28 (10)	2.8
	33	72 (1)	54 (2)	18 (2)	9.0
	12	9 (2)	2 (5)	7 (5)	
	13	42 (1)	31 (2)	11 (2)	
	23	4 (2)	−27 (4)	31 (4)	
N(3)	11	155 (2)	121 (3)	34 (4)	8.5
	22	354 (4)	294 (9)	60 (10)	6.0
	33	98 (1)	89 (2)	9 (2)	4.5
	12	−66 (3)	−75 (5)	11 (6)	
	13	50 (1)	38 (2)	12 (2)	
	23	−21 (2)	−24 (4)	3 (4)	
C(6)	11	100 (2)	88 (3)	12 (4)	3.0
	22	198 (3)	171 (8)	26 (9)	2.9
	33	55 (1)	40 (2)	15 (2)	7.5
	12	−9 (2)	−13 (5)	4 (4)	
	13	20 (1)	18 (2)	2 (2)	
	23	2 (1)	1 (4)	1 (4)	

[a] The atom numbering is that used in ref 3.

Conclusion

We have demonstrated the usefulness of combined X-ray and neutron scattering experiments for the experimental study of electron charge density distributions in molecular crystals and specifically in TCEO, where strong evidence has been obtained for the existence of a bent endocyclic C–C bond. Additional studies of these densities in both real and reciprocal space are currently in progress in order to compare independently measured functions of charge density distributions such as the dipole moment with those calculated from our experiments.

Electrogenerated Chemiluminescence. V. The Rotating-Ring–Disk Electrode. Digital Simulation and Experimental Evaluation

J. T. Maloy, Keith B. Prater, and Allen J. Bard*[1]

Contribution from the Department of Chemistry, The University of Texas at Austin, Austin Texas 78712.
Received January 13, 1971

Abstract: The rotating-ring–disk electrode (rrde) was used to generate the radical ion precursors of electrogenerated chemiluminescence (ecl). A cell assembly was designed to allow solutions to be degassed under vacuum and allowed the rrde to function in an inert atmosphere with the simultaneous performance of electrochemical and spectroscopic experiments. Digital simulation techniques have been employed to treat ecl at the rrde. The simulations predict the effect of rrde rotation rate and the kinetics of the radical ion annihilation reaction on the intensity of ecl light. When this annihilation reaction is very fast, *i.e.*, greater than $10^7\ M^{-1}\ \text{sec}^{-1}$ for the rrde used here, the ecl is seen as a sharp ring of light at the inner edge of the ring electrode, and its intensity, like the disk current, is proportional to the square root of rotation rate. The simultaneous measurement of steady-state disk current and ecl intensity as functions of the disk potential gives direct information about the role of any disk-generated species in the light-producing process. An evaluation of the technique using the ecl of 9,10-diphenylanthracene in *N*,*N*-dimethylformamide solution is described.

Electrogenerated chemiluminescence (ecl) studies are usually carried out at a single working electrode whose potential is varied to generate the reduced and oxidized species which react in the diffusion layer near the electrode to produce light.[2] While this method is simple experimentally and has been very useful in the elucidation of reaction mechanisms in ecl, it suffers from several disadvantages. Because of the repetitive switching at a single electrode, a fraction of the species produced during one half-cycle is consumed electrochemically during the next half-cycle. This makes it

(1) To whom correspondence and requests for reprints should be directed.

(2) This work has been reviewed in (a) A. J. Bard, K. S. V. Santhanam, S. A. Cruser, and L. R. Faulkner, "Fluorescence," G. G. Gullbault, Ed., Marcel Dekker, New York, N. Y., 1967, Chapter 4; (b) D. M. Hercules, *Accounts Chem. Res.*, 2, 301 (1969).